CrossMark

Can MDCT or EUS features predict the histopathological grading scheme of pancreatic neuroendocrine neoplasms?

Hui Zhu[1,2] · Lang Ying[3] · Wei Tang[1,2] · Xiujiang Yang[2,4] · Bo Sun[2,4]

Abstract

Purpose To identify whether the features of preoperative MDCT or EUS could predict the histopathological grading scheme of pancreatic neuroendocrine neoplasms (pNENs).

Methods A total of 25 patients with pNENs were enrolled in the present study. The qualitative and quantitative variables were reviewed. The qualitative variables included location, contour, border, necrosis, intratumoral vessel, homogeneity, calcification, peripancreatic fat/vessel infiltration, pancreatic duct dilatation, mass within pancreas, lymphadenopathy and hepatic metastasis on MDCT and border, echogenicity, cystic/solid and blood flow on EUS. The quantitative variables included long diameter (LD), short diameter (SD), unenhanced mass attenuation (UMA), unenhanced pancreatic attenuation (UPA), arterial phase mass attenuation (APMA), arterial phase pancreatic attenuation (APPA), portal venous phase mass attenuation (PVPMA), portal venous phase pancreatic attenuation (PVPPA), arterial phase enhancement degree (APED) and portal venous phase enhancement degree (PVPED). In addition, sex and age were also evaluated. Histopathological classifications met the criterion of 2010 edition WHO Histopathological Classifications. Kruskal–Wallis test and Boruta algorithm were conducted.

Results Lymphadenopathy and peripancreatic fat or vascular invasion foretold higher histopathological grading level while well-defined border on EUS image lower grading level.

Conclusions Lymphadenopathy, border on EUS image and peripancreatic fat or vascular invasion can predict the histopathological grading scheme of pNENs.

Keywords Multi-detector computed tomography (MDCT) · Endosonography · Pancreatic neuroendocrine neoplasms · Pathological classification · Prognosis

H. Zhu and L. Ying contributed equally to this work.

✉ Bo Sun
gidrsunbo@126.com

1 Department of Radiology, Fudan University Shanghai Cancer Center, Shanghai, China

2 Department of Oncology, Shanghai Medical College, Fudan University, 270 DongAn Road, Shanghai 200032, China

3 Department of Orthopaedics, Yancheng Third People's Hospital, The Affiliated Yancheng Hospital of Southeast University Medical College, 75 JuChang Road, Yancheng 224001, China

4 Department of Endoscopy, Fudan University Shanghai Cancer Center, Shanghai, China

Introduction

Pancreatic neuroendocrine neoplasms (pNENs) are rare neoplasms which comprise 1–2% of pancreatic neoplasms [1]. A large population study based on the Surveillance, Epidemiology, and End Results (SEER) database showed that the crude annual incidence was only 1.8 per 1,000,000 in females while 2.6 in males and increased with advancing age [2]. Although their infrequency, pNENs are still focused by researchers because they have distinct therapeutic strategies (both medical and surgical) and better prognosis compared to pancreatic ductal adenocarcinomas [3, 4]. There has been an increase in its detection rate, which is attributed to the technical progress of modern imaging modalities such as multi-detector computed tomography (MDCT), endoscopic ultrasound (EUS) and EUS-guided fine-needle aspiration (EUS-FNA). It was reported that mean detection rate, sensitivity and specificity of CT scan

in diagnosis pNENs were 73, 73 and 96%, respectively [5]. And EUS-FNA was considered as an effective tool which provides high-resolution images of pancreas through the wall of the gastrointestinal tract and obtains cytological findings and immunocytochemical stains to make the accurate identification of pNENs [6, 7]. Previous study showed the sensitivity of EUS-FNA for the diagnosis of this entity was 87% [8]. Therefore, current guidelines recommend MDCT and EUS as the initial imaging modalities for the initial work-up for suspected pNENs [9–11]. Histopathologically, 2010 World Health Organization (WHO) classification divides pNENs into grade 1 (G1), grade 2 (G2) and grade 3 (G3, i.e., neuroendocrine carcinoma) according to a grading scheme based on mitotic count or Ki67 index [12]. To optimize surgical management, correct preoperative predicting histopathological classifications of pNENs is ideal. The goal of this study was to identify whether the features of preoperative MDCT or EUS could predict the histopathological grading scheme of pNENs.

Materials and methods

Study population

This retrospective study was approved by our institutional review board, and informed consent was waived. We reviewed cross-referenced records in the departments of radiology, endoscopy and pathology in our hospital from July 2012 to June 2015. To develop a study group of suitable cases for identifying which features of MDCT or EUS could predict the histopathological classifications of pNENs, we used the following inclusion criteria: histopathologically confirmed PNENs, available clinicopathologic data (including sex, age and 2010 edition WHO grading data), available unenhanced and contrast -enhanced (both the arterial phase and portal venous phase) CT images, available EUS images. Patients who had already received surgery, chemotherapy or radiotherapy prior to the study were excluded from the study.

MDCT technique

Immediately before scanning, 500–800 mL of negative or positive contrast agent was administered orally to all patients to distend the gastrointestinal tract. MDCT protocols included unenhanced and contrast-enhanced CT (both the arterial phase and the portal venous phase) scan by using different scanners (SOMATOM Sensation 40 and SOMATOM Sensation 64; Siemens AG, Medical Solutions, Business Unit CT, Forchheim, Germany). With the use of a power injector (Ulrich Medizintechnik, Buchbrunnenweg, Germany), 100–120 mL of nonionic contrast

agent (iopamidol, 300 mg iodine/mL, Iopamiro; Bracco Sine, Shanghai, China or iohexol, 300 mg iodine/mL, Omnipaque 300; Amersham, Shanghai, China) was administrated (at the rate of 3 mL/s, with a 30- or 60-s delay for arterial phase or portal vein phase, respectively) via a intravenous catheter into a vein in the elbow. The MDCT scanning was performed during inspiratory breath hold. The parameters for the CT examinations were as follows: tube voltage, 120 kV; tube current, 250 mA; slice thickness, 3 mm. The original images uploaded to the picture archiving and communication system (PACS, GE Healthcare-Centricity RIS CE V2.0; GE Medical Systems, Fairfield, Conn).

EUS technique

All EUS procedures were performed by two experienced endosonographers (X. J. Y. and B. S., with 15 and 10 years of EUS practice, respectively) using a GF-UCT 260 (Olympus, Japan) curve linear echoendoscope with an Aloka ultrasound processor (Aloka alpha 10, Tokyo, Japan) or an EG-3870UTK (Pentax, Japan) curve linear echoendoscope with a Hitachi ultrasound scanning system (Hitachi Preirus, Japan). Conscious sedation was provided to all study patients with intravenous midazolam and fentanyl. Doppler imaging was used to identify blood vessels during the procedures. The original images were uploaded to the PACS (GE Healthcare-Centricity RIS CE V2.0; GE Medical Systems, Fairfield, Conn).

MDCT image analysis

MDCT images were presented to two experienced abdominal radiologists (H. Z. and W. T., with 24 and 9 years of radiology practice, respectively) in a random sequence through PACS. The radiologists evaluated the qualitative and quantitative variables who were blind to the histopathological classifications and EUS results. The qualitative variables included the location (head, body or tail; pancreatic head is on the right of the superior mesenteric-portal vein confluence while pancreatic body is between the left edge of the superior mesenteric–portal vein confluence and the left edge of the aorta; pancreatic tail is those arising to the left of the left edge of the aorta.) contour (round, oval, lobulated or irregular), border on MDCT(B (MDCT), well-defined or ill-defined), necrosis (present or absent; the intra-lesional low attenuation is considered as necrosis at a CT value of <20 HU), intratumoral vessel (IV, present or absent), homogeneity (yes or no), calcification (present or absent), peripancreatic fat/vessel infiltration (FVI, present or absent; peripancreatic/perivascular fat plane disappears or vessel deforms), pancreatic duct dilatation (PDD, present or absent), mass within pancreas (WP, yes or no, mass confined within the

margin of pancreatic tissue without extension beyond the margin), lymphadenopathy (short diameter of lymph node >10 mm, present or absent) present or absent) and hepatic metastasis (HM, present or absent). All of these qualitative variables were evaluated on arterial or portal venous phase depending upon optimal visualization. The quantitative variables included long diameter of mass (LD, expressed in millimeter), short diameter of mass (SD, expressed in millimeter), unenhanced mass attenuation (UMA, expressed in CT value HU), unenhanced pancreatic attenuation (UPA, expressed in CT value HU), arterial phase mass attenuation (APMA, expressed in CT value HU), arterial phase pancreatic attenuation (APPA, expressed in CT value HU), portal venous phase mass attenuation (PVPMA, expressed in CT value HU), portal venous phase pancreatic attenuation (PVPPA, expressed in CT value HU), arterial phase mass enhancement degree (APED, APMA minus UMA, expressed in CT value HU) and portal venous phase mass enhancement degree (PVPED, PVPMA minus UMA, expressed in CT value HU). Discrepancies between the radiologists were resolved by consensus after reevaluation together.

EUS image analysis

EUS images were presented to two experienced endosonographers (X. J. Y. and B. S., with 15 and 10 years of EUS practice, respectively) in a random sequence through PACS who were blind to the histopathological classifications and MDCT results. Border on EUS (B (EUS), well-defined or ill-defined), echogenicity (hyperechoic, iso-echoic or hypoechoic), cystic/solid (CS; solid, cystic or mixed solid and cystic), and abundant blood flow (yes or no) were evaluated. Discrepancies between the endosonographers were also resolved by consensus after reevaluation together. Furthermore, sex and age were also analyzed.

WHO histopathological classifications

Each pathological report met the criterion of 2010 edition WHO Histopathological Classifications based on mitotic count or Ki67 index. pNENs with mitotic count <2 per 10 high-power fields (HPF) and/or Ki67 index ≤2% was graded as Grade 1 (G1), pNENs with mitotic count 2–20 per 10 HPF and/or Ki67 index 3–20% was graded as Grade 2 (G2) and pNENs with mitotic count >20 per 10 HPF and/ or Ki67 index >20% was graded as Grade 3 (G3).

Statistical analysis

The inter-rater agreement (for qualitative data) was estimated by using Kappa statistic. The strength of agreement was determined by the value of Kappa (<0.20, poor; 0.21–0.40, fair; 0.41–0.60, moderate; 0.61–0.80, good; 0.81–1.00,

very good). The reliability of measurements or ratings (for quantitative data) was estimated using intra-class correlation coefficient. As for intra-class correlation coefficient, the criteria were as below: <0.10, virtually none; 0.11–0.40, slight; 0.41–0.60, fair; 0.61–0.80, moderate; 0.81–1.00, substantial. The relation between MDCT, EUS, sex or age (including qualitative and quantitative variables) and histopathological grading scheme of pNENs was analyzed using Kruskal–Wallis test. The analysis was conducted by using MedCalc statistical software Version 11.4.2.0 (MedCalc Software bvba, Acacialaan 22, 8400 Ostend, Belgium). In addition, Feature selection (Boruta algorithm) was also performed to identify the most important attributes that were independently associated with the histopathological grading scheme of pNENs. This algorithm was a wrapper built around the Random Forest classification algorithm implemented in R program (www.r-project.org/) Random Forest [13, 14]. With this method we could clearly identify which MDCT or EUS features were the most important attributes that were associated with the histopathological grading scheme, independently of each other.

Results

A total of 25 patients with pNENs (13 males and 12 females; mean age, 54.6 years; age range, 26–75 years) were enrolled in the present study. Each patient had solitary lesion. There were nine patients diagnosed as G1, eleven patients G2 and five patients G3. The values of Kappa suggested that the agreement between two radiologists was good or very good: B (EUS), 0.84; B (MDCT), 0.84; blood flow, 0.76; calcification 0.83; contour, 0.83; CS, 0.78; echo, 0.70; FVI, 0.84; HM, 0.72; homogeneity, 0.75; IV, 0.75; location, 0.75; lymphadenopathy, 0.80; necrosis, 0.82; PDD, 0.78; WP, 0.75. The results of intra-class correlation coefficient showed that the reliability of measurements or ratings was substantial: UMA, single measure 0.82, average measure 0.90; UPA, single measure 0.94, average measure 0.97; APMA, single measure 0.85, average measure 0.92; APPA, single measure 0.99, average measure 0.99; PVPMA, single measure 0.98, average measure 0.99; PVPPA, single measure 0.95, average measure 0.98; APED, single measure 0.83, average measure 0.91; PVPED, single measure 0.96, average measure 0.98; LD, single measure 0.99, average measure 0.99; SD, single measure 0.99, average measure 1.00. We adopted the results estimated by H. Z. as the final results.

Qualitative analysis by Kruskal–Wallis test

Qualitative analysis by Kruskal–Wallis test for MDCT or EUS features are summarized in Table 1. G3 pNENs were

Table 1 Qualitative analysis according to histopathological grading scheme

Qualitative variable	G1 ($n = 9$)	G2 ($n = 11$)	G3 ($n = 5$)	p value*
Sex				0.3893
Male	4 (44.44)	5 (45.45)	4 (80.00)	
Female	5 (55.56)	6 (54.55)	1 (20.00)	
Location				0.2676
Head	4 (44.44)	5 (45.45)	4 (80.00)	
Body	3 (33.33)	1 (9.09)	1 (20.00)	
Tail	2 (22.22)	5 (45.45)	0 (0.00)	
Contour				0.4861
Round	4 (44.44)	1 (9.09)	2 (40.00)	
Oval	1 (11.11)	3 (27.27)	0 (0.00)	
Lobulated	3 (33.33)	5 (45.45)	2 (40.00)	
Irregular	1 (11.11)	2 (18.18)	1 (20.00)	
B(MDCT)				0.0614
Well-defined	6 (66.67)	5 (45.45)	0 (0.00)	
Ill-defined	3 (33.33)	6 (54.55)	5 (100.00)	
Necrosis				0.2526
Absent	8 (88.89)	6 (54.55)	3 (60.00)	
Present	1 (11.11)	5 (45.45)	2 (40.00)	
IV				0.6785
Absent	8 (88.89)	8 (72.73)	4 (80.00)	
Present	1 (11.11)	3 (27.27)	1 (20.00)	
Homogeneity				0.1305
No	3 (33.33)	8 (72.73)	4 (80.00)	
Yes	6 (66.67)	3 (27.27)	1 (20.00)	
Calcification				0.1246
Absent	9 (100.00)	8 (72.73)	5 (10.00)	
Present	0 (0.00)	3 (27.27)	0 (0.00)	
FVI				0.0232†
Absent	7 (77.78)	5 (45.45)	0 (0.00)	
Present	2 (22.22)	6 (54.55)	5 (100.00)	
PDD				0.1565
Absent	9 (100.00)	8 (72.73)	3 (60.00)	
Present	0 (0.00)	3 (27.27)	2 (40.00)	
WP				0.0373†
Absent	3 (33.33)	8 (72.73)	5 (100.00)	
Present	6 (66.67)	3 (27.27)	0 (0.00)	
Lymphadenopathy				0.0074†
Absent	9 (100.00)	8 (72.73)	1 (20.00)	
Present	0 (0.00)	3 (27.27)	4 (80.00)	
HM				0.0707
Absent	9 (100.00)	6 (54.55)	3 (60.00)	
Present	0 (00.00)	5 (45.45)	2 (40.00)	
B(EUS)				0.0079†
Well-defined	8 (88.89)	2 (18.18)	2 (40.00)	
Ill-defined	1 (11.11)	9 (81.82)	3 (60.00)	
CS				0.2650
Solid	9 (100.00)	9 (81.82)	5 (100.00)	

Table 1 continued

Qualitative variable	G1 ($n = 9$)	G2 ($n = 11$)	G3 ($n = 5$)	p value*
Cystic or mixed solid	0 (0.00)	2 (18.18)	0 (0.00)	
Cystic	0 (0.00)	0 (0.00)	0 (0.00)	
Echogenicity				0.5284
Hypoechoic	6 (66.67)	10 (90.91)	5 (100.00)	
Isoechoic	3 (33.33)	1 (9.09)	0 (0.00)	
Hyperechoic	0 (0.00)	0 (0.00)	0 (0.00)	
Abundant bloodflow				0.7961
No	3 (33.33)	5 (45.45)	3 (60.00)	
Yes	6 (66.67)	6 (54.55)	2 (40.00)	

Data are numbers of patients, with percentages in parentheses. Percentages may not add up to 100% because of rounding

B(MDCT) border (MDCT), *FVI* fat or vascular invasion, *PDD* pancreatic duct dilatation, *WP* mass within pancreas, *HM* hepatic metastasis, *B(EUS)* border (EUS), *CS* cystic/solid

* Calculated with Kruskal–Wallis test

† Significant values

Table 2 Quantitative analysis according to histopathological grading scheme

Quantitative variable	Mean	Std dev	p value*
UMA	40.92	5.90	0.8649
UPA	41.56	9.39	0.4175
APMA	124.32	57.20	0.0722
APPA	86.80	29.30	0.2008
PVPMA	102.64	25.67	0.7906
PVPPA	82.88	18.32	0.6043
APED	83.40	56.40	0.0626
PVPED	61.72	25.48	0.8461
LD	40.72	25.92	0.1018
SD	32.64	21.19	0.1318
Age	54.60	10.96	0.0077†

Std Dev standard deviation, *UMA* unenhanced mass attenuation, *UPA* unenhanced pancreatic attenuation, *APMA* arterial phase mass attenuation, *APPA* arterial phase pancreatic attenuation, *PVPMA* portal venous phase mass attenuation, *PVPPA* portal venous phase pancreatic attenuation, *APED* arterial phase enhancement degree, *PVPED* portal venous phase enhancement degree, *LD* long diameter, *SD* short diameter

* Calculated with Kruskal–Wallis test

† Significant values

apt to break through the pancreatic capsule ($p < 0.05$) and none of G3 pNENs were within pancreas in our study. Accordingly, peripancreatic fat or vascular invasion was more common in G3 pNENs ($p < 0.05$) and all of G3 masses presented this sign. More G3 pNENs (80%) were associated with lymphadenopathy ($p < 0.01$). On EUS
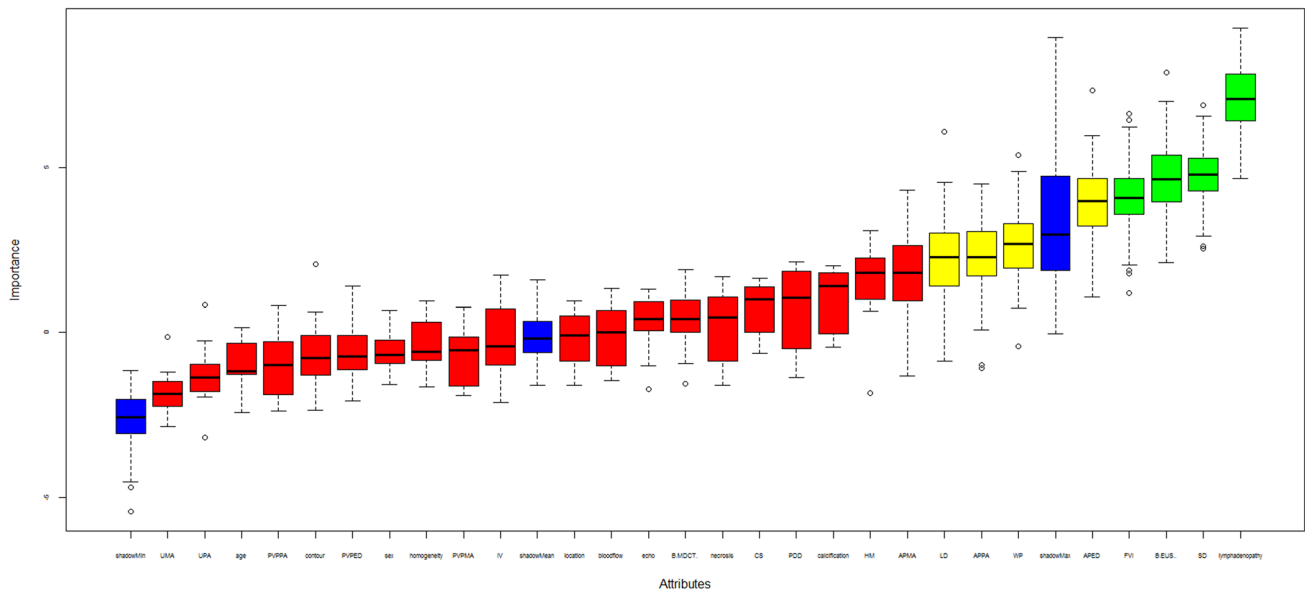
Fig. 1 Feature selection analysis (Boruta algorithm) to identify variables most closely related to the histopathological grading scheme of pNENs. All the qualitative and quantitative variables were ranked as possible determinants of the histopathological grading. *Green* columns (lymphadenopathy, SD, B.EUS. and FVI) were confirmed as being "important" attributes for the histopathological grading scheme of pNENs. *Yellow* columns (WP, APPA, APMA and PDD) represent "tentative" attributes whereas *red* (HM, LD, BMDCT, echo, necrosis, CS, age, IV, bloodflow, homogeneity, calcification, sex, contour, PVPPA, UMA, PVPMA, location, UPA) "rejected". *Blue* columns represent "shadow attributes". The *Y* axis represents the value of importance (mean, median, minimum, and maximum Z). *APMA* arterial phase mass attenuation, *APPA* arterial phase pancreatic attenuation, *CS* cystic/solid, *FVI* fat or vascular invasion, *HM* hepatic metastasis, *IV* intratumoral vessel, *LD* long diameter, *PDD* pancreatic duct dilatation, *PVPMA* portal venous phase mass attenuation, *PVPPA* portal venous phase pancreatic attenuation, *SD* short diameter, *UMA* unenhanced mass attenuation, *UPA* unenhanced pancreatic attenuation, *WP* within pancreas

images, well-defined masses (88.89%) were significantly more prevalent in G1 pNENs ($p < 0.001$). Other 13 qualitative image features (sex, location, contour, border on MDCT images, necrosis, intratumoral vessel, homogeneity, calcification, pancreatic duct dilatation, hepatic metastasis, echogenicity, cystic/solid and blood flow) had no significant difference among three histopathological grading levels ($p > 0.05$).

Quantitative image analysis by Kruskal–Wallis test

Only one quantitative feature (age) had significant difference among three histopathological grading levels ($p < 0.01$). Ten other quantitative image features (LD, SD, UMA, UPA, APMA, APPA, PVPMA, PVPPA, APED and PVPED) were no significant difference among three histopathological grading levels ($p > 0.05$). These results were listed in Table 2.

Boruta algorithm for qualitative or quantitative analysis

Boruta algorithm confirmed that four features (lymphadenopathy, SD, border on EUS image and peripancreatic fat

or vascular invasion) were confirmed important in related to histopathological grading levels. Four features (APED, APPA, LD and mass within pancreas) were identified tentative and 20 features (age, sex, location, contour, necrosis, homogeneity, echo, calcification, intratumoral vessel, hepatic metastasis, border on MDCT image, blood flow, CS, UMA, PPD, UPA, APMA, PVPMA, PVPED and PVPPA) unimportant. The results of Boruta algorithm are presented in Fig. 1.

Combined with results of aforementioned two statistical tests, we found that three features, lymphadenopathy, border on EUS image and peripancreatic fat or vascular invasion, related to the histopathological grading scheme-namely, presenting lymphadenopathy and peripancreatic fat or vascular invasion were inclined to higher histopathological grading level (Fig. 2) while well-defined border on EUS image indicated lower (Fig. 3).

Discussion

It is of great significance to evaluate pNENs preoperatively because they were considered as potential malignancy [15]. Several imaging modalities, including

Fig. 2 A G3 pNEN in a 59-year-old man. Axial contrast-enhanced CT scans (**a** arterial phase; **b** portal venous phase) depict peripancreatic fat infiltration (*arrows*) adjacent to the mass in the head of pancreas. The *lower* level image (**c** portal venous phase) shows retroperitoneal lymphadenopathy (*stars*). **d** EUS demonstrates a hypoechoic solid mass in the head of pancreas with ill-defined border (*arrows*)
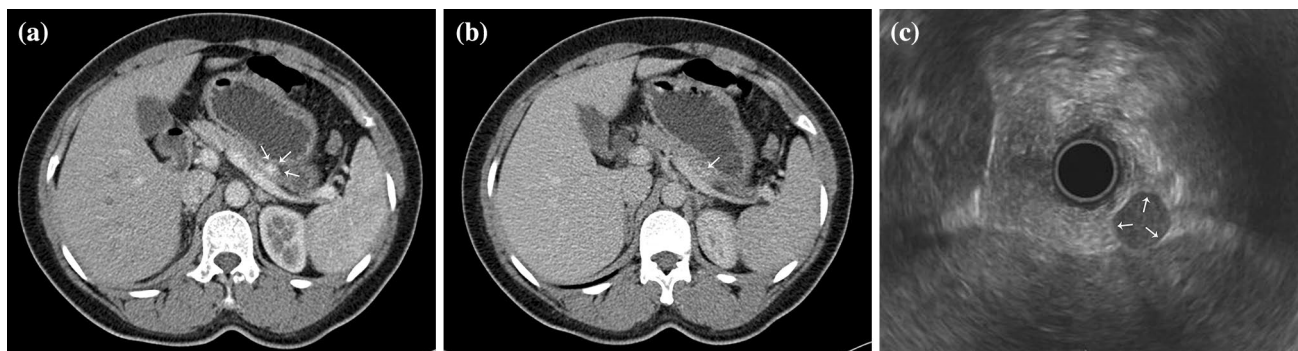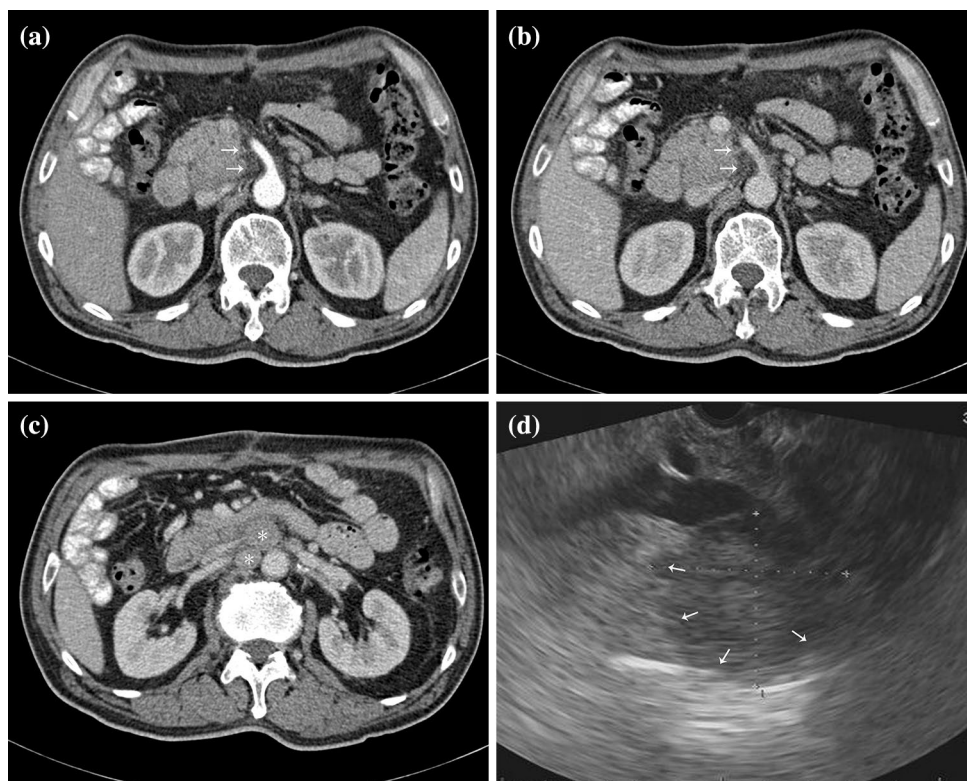

Fig. 3 A G1 pNEN in a 43-year-old woman. **a** Axial arterial phase contrast-enhanced CT scans depict enhancing nodule in the tail of pancreas (*arrows*). **b** The nodule (*arrow*) on axial portal venous phase contrast-enhanced CT scans is poorly enhancing. **c** EUS demonstrates a hypoechoic solid mass in the tail of pancreas with well-defined border (*arrows*)

morphological imaging (MDCT, MRI or EUS) and functional imaging (SPET or PET-CT), are often used as preoperative detection, localization or diagnostic workup for suspected pNENs [16–20]. Some studies evaluated the value of diffusion-weighted imaging in prediction of the histologic grade of pNENs. Jang et al. found that ADC values and ADC ratios of tumor to pancreas (ADC value of tumor/ADC value of pancreas) in patients with benign pNEN (mean, 1.48×10^{-3} mm^2/s, 1.11 ± 0.25, each) were higher than those in patients with non-benign pNEN (mean, 1.04×10^{-3} mm^2/s, 0.74 ± 0.13, each) [21]. Another study using intravoxel incoherent motion (IVIM)

diffusion-weighted imaging showed that there were lower pure diffusion coefficients (D values) in grade 2 and 3 than those in grade 1 (0.95 vs 1.21×10^{-3} mm^2/s; $p = 0.009$) and pure diffusion coefficient (D) was possibly a better index than ADC (total) was in differentiating grade 1 from grade 2 or 3 pNEN [22]. Furthermore, several researchers used positron emission tomography (PET) in predicting grade in pNENs. The SUV_{max} of G3 was higher than that of G1/G2 (5.0 ± 2.5 vs. 2.7 ± 1.6). Using 2.5 as a cutoff value of SUV_{max}, the sensitivity, specificity, and accuracy of differentiating G3 tumors from G1/G2 were 100.0, 62.5 and 66.7%, respectively [23].

As for a noninvasive technique, MDCT is the most widely modality for primary tumor, metastases or recurrence, owing to its high spatial and temporal resolution [19, 24]. It can acquire data quickly, create multiplanar reformation by images postprocessing and display images in the desired planes. EUS, a minimally invasive method, can depict smaller lesion invisible on other imaging methods because its higher frequency probe can position in proximity to the pancreas [25]. Furthermore, EUS-FNA can obtain histological diagnosis with high accuracy as part of the preoperative evaluation, which is applied to not primary pancreatic lesions, but also peripancreatic lymphatic metastases [26, 27]. Based on the above-mentioned advantages, MDCT and EUS are popular assessment approaches for pNENS.

According to our results, well-defined border on EUS image indicated lower histopathological grading (tending to be benign), whereas lymphadenopathy and peripancreatic fat or vascular invasion were inclined to higher histopathological grading (tending to be malignant). These findings were partially consistent with the previous studies: Gallotti A reported that presence of vascular invasion, lymph node enlargement or pancreatic duct dilatation was more highly related to non-benign lesions than to benign tumors [28]. In another study from Luo, however, univariate analysis suggested eight CT features (size, contour, cystic necrosis, boundary, dilatation of the main pancreatic duct, peripancreatic tissue or vascular invasion, lymphadenopathy and distant metastasis) had statistically significant differences among the histopathological grading of pNENs while multivariate analysis revealed that only one CT feature (peripancreatic tissue or vascular invasion) was significantly associated with the histopathological grading [29]. In the latter study, we noticed that tumor size had different statistical results in univariate analysis but not in multivariate analysis. This phenomenon was also observed in our series: SD (short diameter of tumor) was associated with histopathological grading in Boruta algorithm but they were irrelevant in Kruskal–Wallis test. In addition, Hwang [22] believed that grades 2 and 3 pNENs were significantly larger than grade 1 tumors and Kishi [30] found that smaller pNENs had little risk of metastases or recurrence. Thus, whether tumor size was correlation with histopathological grading is a debatable point and need be validated by larger sample sizes. As for enhancement features of pNENs, some researchers [31] found that hypoenhancing pNENs on arterial phase had significantly worse overall survival after a resection and proved it to be an independent predictor of poor prognosis. These tumors with biological aggressiveness were inclined to lymph node or liver metastases. In our cohort, however, enhancement features did not predict whether the lesions were benign or malignant. We speculated that this inconformity maybe ascribed to different contrast enhancement scan protocols used.

There were several limitations to our study. To start with, various CT scanners and nonionic contrast agents were used in the present study because this retrospective study had no designated scanner and contrast agent. And secondly EUS elastography data were not adopted owing to incomplete records. Although these defects, we believe our findings may be helpful in predicting the histopathological grading and in planning individualized treatment for pNENs.

In conclusion, three features of MDCT or EUS can predict the histopathological grading scheme of pNENs-lymphadenopathy, peripancreatic fat or vascular invasion or border on EUS image. Lymphadenopathy and peripancreatic fat or vascular invasion are inclined to malignancy whereas well-defined border on EUS image indicates benign tumor.

References

1. Oberg K, Eriksson B (2005) Endocrine tumours of the pancreas. Best Pract Res Clin Gastroenterol 19:753–781
2. Halfdanarson TR, Rabe KG, Rubin J et al (2008) Pancreatic neuroendocrine tumors (PNETs): incidence, prognosis and recent trend toward improved survival. Ann Oncol 19:1727–1733
3. Chen H, Hardacre JM, Uzar A et al (1998) Isolated liver metastases from neuroendocrine tumors: does resection prolong survival. J Am Coll Surg 187:88–92
4. Karaman K, Bostanci EB, Aksoy E et al (2011) The predictive value of mean platelet volume in differential diagnosis of nonfunctional pancreatic neuroendocrine tumors from pancreatic adenocarcinomas. Eur J Intern Med 22:e95–e98
5. Sundin A, Vullierme MP, Kaltsas G et al (2009) ENETS Consensus Guidelines for the Standards of Care in Neuroendocrine Tumors: radiological examinations. Neuroendocrinology 90:167–183
6. Maletta F, Pacchioni D, Carucci P et al (2011) Analysis of cyst fluid obtained by endoscopic ultrasound-guided fine-needle aspiration supporting the diagnosis of a pancreatic neuroendocrine neoplasm. Endoscopy 43(Suppl 2 UCTN):E34–E35
7. Larghi A, Capurso G, Carnuccio A et al (2012) Ki-67 grading of nonfunctioning pancreatic neuroendocrine tumors on histologic

samples obtained by EUS-guided fine-needle tissue acquisition: a prospective study. Gastrointest Endosc 76:570–577

8. Pais SA, Al-Haddad M, Mohamadnejad M et al (2010) EUS for pancreatic neuroendocrine tumors: a single-center, 11-year experience. Gastrointest Endosc 71:1185–1193

9. Jensen RT, Cadiot G, Brandi ML et al (2012) ENETS Consensus Guidelines for the management of patients with digestive neuroendocrine neoplasms: functional pancreatic endocrine tumor syndromes. Neuroendocrinology 95:98–119

10. Falconi M, Bartsch DK, Eriksson B et al (2012) ENETS Consensus Guidelines for the management of patients with digestive neuroendocrine neoplasms of the digestive system: well-differentiated pancreatic non-functioning tumors. Neuroendocrinology 95:120–134

11. Kulke MH, Benson AB 3rd, Bergsland E et al (2012) Neuroendocrine tumors. J Natl Compr Canc Netw 10:724–764

12. Bosman F Carneiro F, Hruban R Theise N (2010) WHO Classification of Tumours of the Digestive System

13. Liaw AWM (2000) Classification and regression by randomForest. R News 2:18–22

14. Kursa MB, Rudnicki WR (2010) Feature selection with the boruta package. J Stat Softw 36:1–13

15. Schott M, Klöppel G, Raffel A et al (2011) Neuroendocrine neoplasms of the gastrointestinal tract. Dtsch Arztebl Int 108:305–312

16. van Essen M, Sundin A, Krenning EP et al (2014) Neuroendocrine tumours: the role of imaging for diagnosis and therapy. Nat Rev Endocrinol 10:102–114

17. Sharma P, Arora S, Mukherjee A et al (2014) Predictive value of 68Ga-DOTANOC PET/CT in patients with suspicion of neuroendocrine tumors: is its routine use justified. Clin Nucl Med 39:37–43

18. Etchebehere EC, de Santos Oliveira A, Gumz B et al (2014) 68Ga-DOTATATE PET/CT, 99mTc-HYNIC-octreotide SPECT/CT, and whole-body MR imaging in detection of neuroendocrine tumors: a prospective trial. J Nucl Med 55:1598–1604

19. Sahani DV, Bonaffini PA, Fernandez-Del CC et al (2013) Gastroenteropancreatic neuroendocrine tumors: role of imaging in diagnosis and management. Radiology 266:38–61

20. James PD, Tsolakis AV, Zhang M et al (2015) Incremental benefit of preoperative EUS for the detection of pancreatic neuroendocrine tumors: a meta-analysis. Gastrointest Endosc 81(848–856):e1

21. Jang KM, Kim SH, Lee SJ et al (2014) The value of gadoxetic acid-enhanced and diffusion-weighted MRI for prediction of grading of pancreatic neuroendocrine tumors. Acta Radiol 55:140–148

22. Hwang EJ, Lee JM, Yoon JH et al (2014) Intravoxel incoherent motion diffusion-weighted imaging of pancreatic neuroendocrine tumors: prediction of the histologic grade using pure diffusion coefficient and tumor size. Invest Radiol 49:396–402

23. Tomimaru Y, Eguchi H, Tatsumi M et al (2015) Clinical utility of 2-[(18)F] fluoro-2-deoxy-D-glucose positron emission tomography in predicting World Health Organization grade in pancreatic neuroendocrine tumors. Surgery 157:269–276

24. Turaga KK, Kvols LK (2011) Recent progress in the understanding, diagnosis, and treatment of gastroenteropancreatic neuroendocrine tumors. CA Cancer J Clin 61:113–132

25. Khashab MA, Yong E, Lennon AM et al (2011) EUS is still superior to multidetector computerized tomography for detection of pancreatic neuroendocrine tumors. Gastrointest Endosc 73:691–696

26. Ridtitid W, Halawi H, DeWitt JM et al (2015) Cystic pancreatic neuroendocrine tumors: outcomes of preoperative endosonography-guided fine needle aspiration, and recurrence during long-term follow-up. Endoscopy 47:617–625

27. Yoon WJ, Daglilar ES, Pitman MB et al (2013) Cystic pancreatic neuroendocrine tumors: endoscopic ultrasound and fine-needle aspiration characteristics. Endoscopy 45:189–194

28. Gallotti A, Johnston RP, Bonaffini PA et al (2013) Incidental neuroendocrine tumors of the pancreas: MDCT findings and features of malignancy. AJR Am J Roentgenol 200:355–362

29. Luo Y, Dong Z, Chen J et al (2014) Pancreatic neuroendocrine tumours: correlation between MSCT features and pathological classification. Eur Radiol 24:2945–2952

30. Kishi Y, Shimada K, Nara S et al (2014) Basing treatment strategy for non-functional pancreatic neuroendocrine tumors on tumor size. Ann Surg Oncol 21:2882–2888

31. Worhunsky DJ, Krampitz GW, Poullos PD et al (2014) Pancreatic neuroendocrine tumours: hypoenhancement on arterial phase computed tomography predicts biological aggressiveness. HPB (Oxford) 16:304–311